Nanoscience and Nanotechnology Letters
Vol. 8, 1–4, 2016

Comparative Study of Heat Treatment on α-MoO_3 Nanorods as an Electrode Material for Lithium Ion Batteries

Joo-Hyung Kim, Young Hwa Jung, Seok-Min Yong, and Do Kyung Kim*

Department of Materials Science and Engineering, Korea Advanced Institute of Science and Technology (KAIST), 291 Daehak-ro, Yuseong-gu, Daejeon 305-701, Republic of Korea

Uniform α-MoO_3 nanorods with the width of 100 nm and the length of 2 μm have been synthesized by facile hydrothermal method. To study the influence of heat treatment on electrochemical properties, the as-synthesized α-MoO_3 nanorods have been calcined at 400 °C for 3 hrs in air, following the characterization of the phase and morphology of α-MoO_3 nanorods by XRD and SEM. The electrochemical characterization of the α-MoO_3 nanorods has conducted for the lithium half-cells in the voltage range from 1.5 V to 3.75 V (vs. Li/Li^+). The first charge/discharge capacities of as-synthesized and heat treated α-MoO_3 were 259/297, 274/307 mAh g^{-1}, respectively. The heat-treated α-MoO_3 nanorods delivers 307 mAh g^{-1} at a rate of 28 mA g^{-1} (0.1 C), and it exhibits the high rate performance compared to as-synthesized α-MoO_3 nanorods. The oxidation states of Mo and O in α-MoO_3 nanorods have measured by XPS to indicate the strong bonding between Mo and O after heat treatment. Our results present that the oxygen ion filled its vacancy and bonded the molybdenum(V) ion, changed to molybdenum(VI) ion after heat-treatment. It helps to form more stable structure for the heat-treated α-MoO_3 nanorods, showing the improved electrochemical performances as an electrode material for LIBs.

Keywords: Molybdenum Trioxide, Hydrothermal Method, Heat Treatment, Lithium-Ion Battery.

1. INTRODUCTION

Rechargeable lithium-ion battery (LIB) is one of the most important parts in portable devices such as cellular phones and laptop computers because of its high energy density and long cycle life in comparison with the other types of rechargeable batteries.[1] Recently, LIB has been applied to Electric vehicles (EVs) and hybrid electric vehicles (HEVs) which require both high energy density and high power density.[2] Therefore, it should be considered that rechargeable LIB with higher capacity as well as high rate capability to meet these requirements.[3]

Various transition metal oxides have been intensively studied as high capacity electrode materials of LIBs in recent years.[4–6] Molybdenum trioxide (α-MoO_3) is one of lithium intercalation materials which lithium ions can be reversibly inserted and extracted electrochemically. It is stable layered orthorhombic structure which makes lithium ions to intercalate in double sheet layers build up by MoO_6 octahedra. Although it shows good structural stability, cycle life and rate characteristics of this material are not good due to low electronic conductivity.[7,8] In order to solve this problem, some researchers have reported several approaches to enhance electrochemical properties of α-MoO_3.[9–11]

Nanostructured materials have been attracted as one of key solutions by reducing dimensions for higher lithium ion de/intercalation rates. Nanostructures provide materials with large surfaces which facilitate electrochemical reaction. From this point of view, nanomaterials with narrow size distribution and uniform morphology are required for lithium insertion host materials. Here, we have synthesized uniform α-MoO_3 nanorods with the width of 100 nm and the length of 2 μm by simple hydrothermal method. Hydrothermal method is one of the most powerful methods for synthesis of nanomaterials. It can be controlled by temperature, pressure, solvent and time for size and morphology of nanomaterials. The as-synthesized α-MoO_3 nanorods are annealed to overcome low crystallinity and the relations between heat treatment and electrochemical performances of α-MoO_3 nanorods are investigated.

*Author to whom correspondence should be addressed.

2. EXPERIMENTAL DETAILS

The α-MoO_3 nanorods were prepared by hydrothermal synthesis. First, Na_2MoO_4–$2H_2O$ was stirred in 15 mL DI-water for 15 mins, then 20 mL 3 M HCl was added and stirred in 20 mL in the mixture. After mixing, 35 mL DI-water is added in the mixture, then the mixture is transferred to 100 mL teflon-lined stainless steel autoclave and hydrothermally treated at 180 °C for 6 hrs. After hydrothermal method, a white colloidal suspension was washed with DI-water and ethanol 3 times respectively and then dried at 80 °C overnight. To remove H_2O hydrated in α-MoO_3 and improve the crystallinity of α-MoO_3, the as-synthesized sample was sintered at 400 °C for 3 hrs.

The X-ray diffraction patterns were obtained on a diffractometer (D/MAX-RB 12KW, RIGAKU, JAPAN) with Cu Kα radiation ($\lambda = 0.15418$ nm) over an angular range of $10° \leq 2\theta \leq 70°$ at a step width of 0.01°. The morphology and crystalline phase of the α-MoO_3 were analyzed by scanning electron microscopy (SEM, XL30, Philips, Netherlands). The electrochemical performance of α-MoO_3 nanorods was evaluated by assembling CR2032-type coin cell with a Li metal as both counter and reference electrode and a polymer membrane separator (Celgard 2400). The organic electrolyte was 1 M $LiPF_6$ in a 1:1 mixture of ethylene carbonate and dimethyl carbonate. The cathode electrode is prepared by 75 wt% of α-MoO_3 nanorods, 17 wt% of carbon black, 8 wt% of polyvinylidene fluoride binder was dissolved in N-methyl-2-pyrrolidone well mixed and then dried at 120 °C for 6 hrs in vacuum. Electrochemical test was performed by a WBCS3000 multi-channel battery cycler (WonaTech, South Korea) and VMP3 potentiostat (BioLogic, France). Cyclic voltammetry (CV) was measured in the voltage range of 1.5 to 3.75 V (vs. Li/Li^+) with a scan rate of 0.5 mV s^{-1} and galvanostatic charge–discharge test was performed in the voltage range of 1.5 to 3.5 V (vs. Li/Li^+) at various current rates from 0.1 to 5 C. X-ray photoelectron spectroscopy (XPS) was performed with a K-alpha (Thermo VG Scientific, USA) using 180° double focusing hemispherical analyzer with Al Kα (1486.65 eV) X-ray radiation under a base pressure of 1.00×10^{-9} Pa. The carbon 1*s* line has been used to calibrate the binding energy scale for the XPS measurements.

3. RESULTS AND DISCUSSION

Figure 1 shows the X-ray diffraction pattern of α-MoO_3 nanorods. The XRD pattern of the α-MoO_3 nanorods is well indexed with α-MoO_3 (JCPDS No. 65-2421) and the corresponding miller indices are presented in Figure 1. Three obvious peaks are detected at $2\theta = 12.65°$, 25.61°, and 38.97° which correspond to the crystal planes of (020), (040), (060), respectively. The intensities of these planes are increased after heat treatment and the crystal planes of (101) and (111) can be detected which indicates the improvement of crystallinity of α-MoO_3.

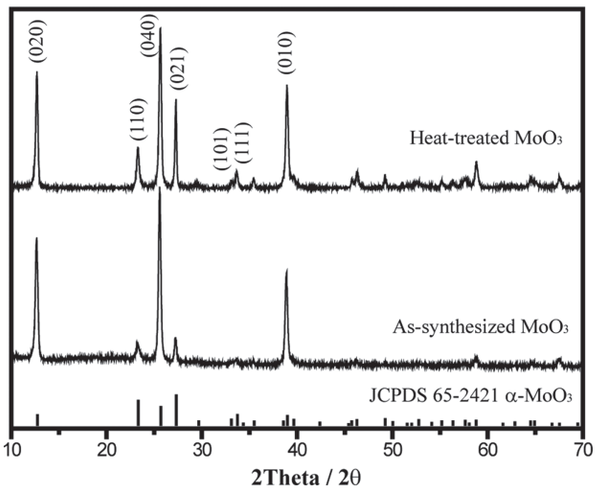

Fig. 1. XRD patterns of α-MoO_3 nanorods before and after heat treatment.

The preferred orientation of (010) plane suggests that the morphology of as-synthesized α-MoO_3 would be a rod-liked shaped one-dimensional (1D) structure. The following SEM micrographs of as-synthesized α-MoO_3 and heat-treated α-MoO_3 in Figure 2 confirm these 1D structures. As-synthesized α-MoO_3 shows a uniform rod-shaped morphology with 2 μm length, 100 nm width. Uniform nanorod-shapes for α-MoO_3 powders were maintained after heat treatment as shown in Figure 2(b).

The electrochemical performance of heat-treated α-MoO_3 nanorods was evaluated by cyclic voltammetry at a scan rate of 0.5 mV s^{-1} in Figure 3(a). In the first cycle, two strong peaks were observed at 2.59 V and 2.08 V in the cathodic reaction while a single peak

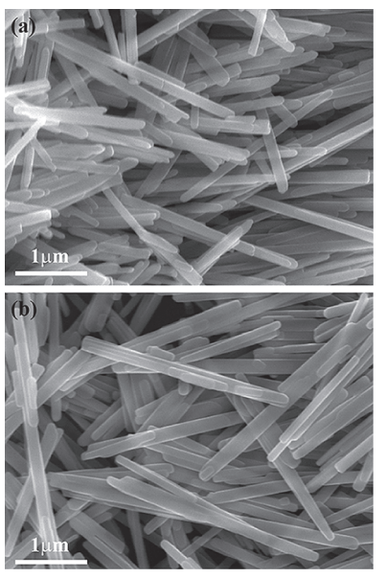

Fig. 2. SEM images of (a) as-synthesized α-MoO_3 nanorods and (b) heat-treated α-MoO_3 nanorods.

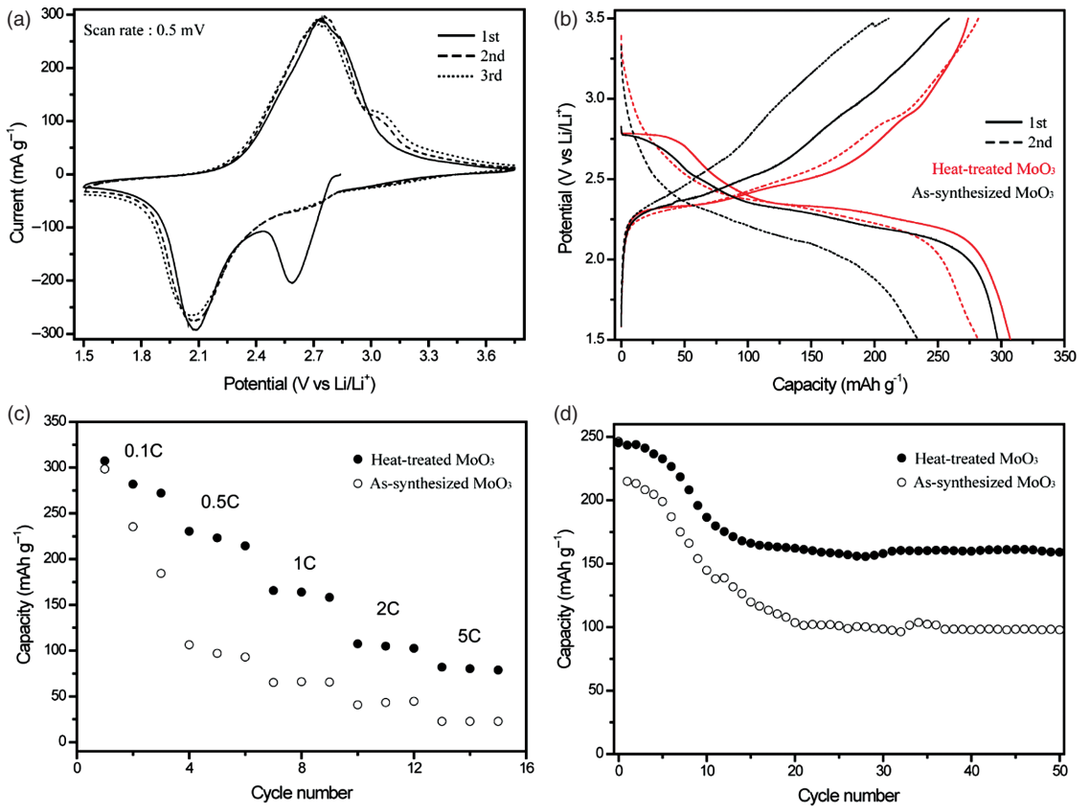

Fig. 3. Electrochemical performances of α-MoO_3 nanorods. (a) Cyclic volammogram of the heat-treated α-MoO_3 nanorods, (b) galvanostatic curves of α-MoO_3 nanorods, (c) rate performances, and (d) cycle performance at 1 C-rate of α-MoO_3 nanorods.

is observed at 2.73 V in the anodic reaction. In the second cycle, the cathodic peak at 2.59 V disappeared, indicating an irreversible reaction between Li ion and MoO_6 octahedral inter/intra-layers at the initial intercalation of Li ions.[7] Disappearance of this peak might be related to a structural modulation that occurs upon insertion/extraction of Li^+ ions. Galvanostatic cycling results also show same behaviors that the first plateau at 2.78 V for heat-treated α-MoO_3 disappeared in the following cycle (Fig. 3(b)). Theoretical capacity of α-MoO_3 is reported about 280 mAh g^{-1}, corresponding to the intercalation of 1.5 Li^+ ion.[12] The first charge/discharge capacities of as-synthesized and heat treated α-MoO_3 were 259/297, 274/307 mAh g^{-1}, respectively (Fig. 3(b)). The discharge capacity loss of heat-treated α-MoO_3 between 1st and 2nd cycle is ca. 26 mAh g^{-1} and that of as-synthesized α-MoO_3 is ca. 63 mAh g^{-1}, indicating the irreversible capacity of α-MoO_3 was decreased after the heat-treatment.

Both α-MoO_3 nanorods were galvanostatically tested with variable current rates from 0.1 to 5 C-rate as shown in Figure 3(c). Upon increasing the discharge rates to 28, 140, 280, 560, and 1400 mA g^{-1}, reversible capacities of as-synthesized α-MoO_3 and heat-treated α-MoO_3 were 297, 107, 68, 49, 25 mAh g^{-1}, and 307, 230, 168, 104, 77 mAh g^{-1}, respectively. Heat-treated α-MoO_3 nanorods show higher rate performance than as-synthesized α-MoO_3 nanorods because of their high crystallinity. The cycling performance was tested under the galvanostatic mode at 1 C-rate in Figure 3(d). As-synthesized and heat-treated α-MoO_3 nanorods in lithium half-cells deliver 243 and 242 mAh g^{-1} of discharge capacity to 1.5 V (vs. Li/Li^+). Discharge capacities for the as-synthesized and heat-treated α-MoO_3 electrodes at 1 C-rate were 39.7 and 65.0% respectively after 50 cycles versus the initial discharge capacity. From the tendency of successive capacities, the heat-treated α-MoO_3 electrode is expected to maintain the reversible discharge capacity of 159 mAh g^{-1} after cycling.

The XPS spectra of both as-synthesized and heat-treated α-MoO_3 were measured to further explain the effect of heat-treatment (Fig. 4). The XPS spectra of both α-MoO_3 nanorods shows Mo $3d_{3/2}$ and $3d_{5/2}$ doublet, which indicates the presence of two types of molybdenum(V, VI) oxo-species. The binding energies of Mo $3d_{3/2}$ and $3d_{5/2}$ doublet in the heat-treated α-MoO_3 are 234.75, 232.08 eV, respectively, which is higher than those of the as-synthesized α-MoO_3. It indicates that oxygen vacancy exists in the as-synthesized α-MoO_3 nanorods and Mo^{6+} ions are more generated after heat treatment.[13, 14] The XPS spectra of α-MoO_3 for O_{1s} also show that the binding energy was 529.28 and 529.07 eV. The binding energy

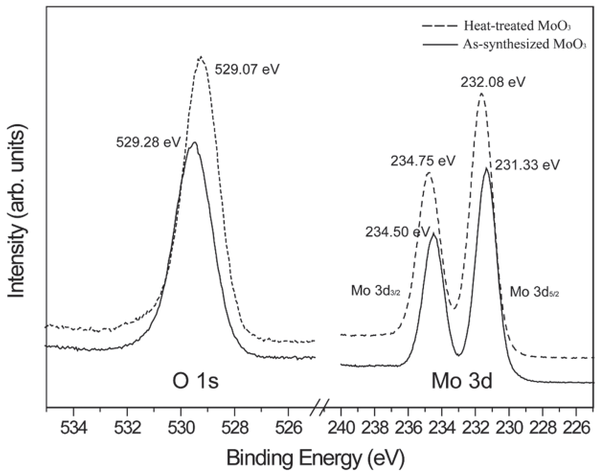

Fig. 4. XPS spectra of α-MoO_3 nanorods for Mo 3*d* and O 1*s* core levels.

of O_{1s} tend to increase as presence of OH groups and association with H_2O.[15] It is important to note that the battery performance is sensitive for H_2O exposure. After heat-treatment, the oxygen ion filled its vacancy and bonded the molybdenum(V) ion, changed to molybdenum(VI) ion, resulting in higher electrochemical performance of the heat-treated α-MoO_3 nanorods.

4. CONCLUSION

We have synthesized the α-MoO_3 nanorods by facile hydrothermal method and conducted a comparative study between the as-synthesized and heat-treated α-MoO_3 nanorods on their electrochemical performances. There is no morphological change of α-MoO_3 nanorods after heat treatment. While the most XRD peak intensity is increased which indicate the improvement of crystallinity of α-MoO_3 nanorods after heat treatment. The heat-treated α-MoO_3 nanorods deliver 307 mAh g^{-1} at a rate of 28 mA g^{-1} (0.1 C) and it exhibits higher rate capability as compared to that of the as-synthesized α-MoO_3 nanorods. The XPS spectrum shows the binding energy of as-synthesized α-MoO_3 nanorods for O_{1s} is related to exposure to H_2O. Furthermore, the binding energy change of Mo $3d_{3/2}$ and $3d_{5/2}$ clear to confirm the increase of oxidation states of molybdenum ions after heat treatment of α-MoO_3. Our study supports that the heat-treated α-MoO_3 nanorods could form more stable structure with less oxygen defects, showing the improved electrochemical performances as an electrode material for LIBs.

Acknowledgments: This work was supported by the Program to Solve Climate Changes (NRF-2010-C1AAA001-2010-0029031) of Korea (NRF) funded by the Ministry of Science, ICT and Future Planning. It was also supported by the Climate Change Research Hub of KAIST (Grant No. N01150034).

References and Notes

1. B. Scrosati, *Nature* 373, 6515 (**1995**).
2. J. M. Tarascon and M. Armand, *Nature* 414, 6861 (**2001**).
3. J. B. Goodenough and K. S. Park, *J. Am. Chem. Soc.* 135, 4 (**2013**).
4. D. K. Kim, P. Muralidharan, H. W. Lee, R. Ruffo, Y. Yang, C. K. Chan, H. Peng, R. A. Huggins, and Y. Cui, *Nano Lett.* 8, 11 (**2008**).
5. Y. H. Jung, D. K. Kim, and S. T. Hong, *J. Power Sources* 233 (**2013**).
6. Y. Li, B. Tan, and Y. Wu, *Nano Lett.* 8, 1 (**2008**).
7. A. M. Hashem, H. Groult, A. Mauger, K. Zaghib, and C. M. Julien, *J. Power Sources* 219 (**2012**).
8. B. Gao, H. Q. Fan, and X. J. Zhang, *J. Phys. Chem. Solids* 73, 3 (**2012**).
9. M. F. Hassan, Z. P. Guo, Z. Chen, and H. K. Liu, *J. Power Sources* 195, 8 (**2010**).
10. T. Tao, A. M. Glushenkov, C. F. Zhang, H. Z. Zhang, D. Zhou, Z. P. Guo, H. K. Liu, Q. Y. Chen, H. P. Hu, and Y. Chen, *J. Mater. Chem.* 21, 25 (**2011**).
11. P. Meduri, E. Clark, J. H. Kim, E. Dayalan, G. U. Sumanasekera, and M. K. Sunkara, *Nano Lett.* 12, 4 (**2012**).
12. S. Berthumeyrie, J. C. Badot, J. P. Pereira-Ramos, O. Dubrunfaut, S. Bach, and P. Vermaut, *J. Phys. Chem. C* 114, 46 (**2010**).
13. R. Tokarz-Sobieraj, K. Hermann, M. Witko, A. Blume, G. Mestl, and R. Schlogl, *Surf. Sci.* 489, 1 (**2001**).
14. K. Kanai, K. Koizumi, S. Ouchi, Y. Tsukamoto, K. Sakanoue, Y. Ouchi, and K. Seki, *Org. Electron.* 11, 2 (**2010**).
15. G. E. Buono-Core, A. H. Klahn, C. Castillo, E. Munoz, C. Manzur, G. Cabello, and B. Chornik, *J. Non-Cryst. Solids* 387 (**2014**).

Received: 8 October 2015. Accepted: 8 December 2015.